Distribution of tsunami interevent times

Eric L. Geist[1] and Tom Parsons[1]

Received 16 November 2007; revised 19 December 2007; accepted 27 December 2007; published 26 January 2008.

[1] The distribution of tsunami interevent times is analyzed using global and site-specific (Hilo, Hawaii) tsunami catalogs. An empirical probability density distribution is determined by binning the observed interevent times during a period in which the observation rate is approximately constant. The empirical distributions for both catalogs exhibit non-Poissonian behavior in which there is an abundance of short interevent times compared to an exponential distribution. Two types of statistical distributions are used to model this clustering behavior: (1) long-term clustering described by a universal scaling law, and (2) Omori law decay of aftershocks and triggered sources. The empirical and theoretical distributions all imply an increased hazard rate after a tsunami, followed by a gradual decrease with time approaching a constant hazard rate. Examination of tsunami sources suggests that many of the short interevent times are caused by triggered earthquakes, though the triggered events are not necessarily on the same fault. **Citation:** Geist, E. L., and T. Parsons (2008), Distribution of tsunami interevent times, *Geophys. Res. Lett.*, *35*, L02612, doi:10.1029/2007GL032690.

1. Introduction

[2] Like other natural hazards, the probability of tsunami occurrence at a particular coastal location depends on both the size distribution of events and the distribution of interevent or recurrence times. Given sufficient historic data, tsunami probability can be determined empirically in which the size distribution tends to follow a truncated or tapered power law distribution [*Burroughs and Tebbens*, 2005]. The interevent distribution for tsunami observations is often assumed to be that of a stationary Poisson process in which interevent times are independent with respect to one another. However, up until now, this assumption has not been tested with tsunami catalog data.

[3] Most coastal locations have an insufficient record of tsunamis, necessitating the use of computational methods as an alternative to empirical tsunami probability determination. For this method, wave heights are computed from numerical tsunami propagation models for all relevant sources and are aggregated together along with their event probabilities [*Geist and Parsons*, 2006]. Similar to the empirical approach, both the size and interevent distributions of sources need to be defined for the computational approach. The size distribution for the most common tsunami generators, earthquakes, follows a power law relation (the modified Gutenberg-Richter law) [e.g., *Kagan*, 2002]. A Poisson process is considered a null hypothesis for earthquake interevent times, with quasiperiodic and clustering models proposed as alternative hypotheses. The dual objectives of this paper, therefore, are to test whether the Poisson assumption for interevent times is valid for tsunami sources (computational approach) and for tsunamis themselves (empirical approach).

[4] Accordingly, we examine two types of datasets for these objectives. The first is a global catalog of tsunami source times. Because it is necessary to have an accurate origin time for this analysis, the catalog consists predominantly of tsunamigenic earthquakes. The second is a catalog of tsunami arrival times at Hilo, Hawaii, chosen because of its long catalog duration. This catalog is used to test the Poisson assumption for empirical probability analyses described above. The majority of the Hilo catalog consists of tsunamis from far-field earthquakes, although local seismogenic tsunamis are also included. Obstacles to this analysis, in comparison to seismicity analysis, is the smaller range of magnitudes of recorded tsunamis and catalog completeness [*Burroughs and Tebbens*, 2005; *Geist and Parsons*, 2006]. Although the Hilo catalog has a smaller sample size compared to the global catalog, it is important to determine the interevent time distribution of tsunamis themselves in comparison to that of global tsunamigenic sources.

2. Empirical Interevent Distribution

[5] Data used to analyze tsunami interevent times are taken from the National Geophysical Data Center (NGDC) tsunami catalog (http://www.ngdc.noaa.gov/seg/hazard/tsu_db.shtml), edited to remove duplicate events and events with inaccurate arrival or origin times. For the Hilo catalog of tsunami arrival times, only tide gage measurements are used for this analysis, since eyewitness observations of arrival time are prone to error. Prior to the devastating Aleutian tsunami of April 1, 1946, the catalog of tsunamis at a detection level of 0.1 m is incomplete, as indicated by plotting the cumulative number of observations since 1900 (Figure 1a) [cf. *Pérez*, 1999]. This can be considered "instrumental censoring" of the observations.

[6] For the global catalog, tsunami source times are given primarily by the hypocentral times of earthquakes. In cases where tsunamigenic aftershocks follow close in space and time (i.e., hours) to the mainshock, only one event may be listed in the NGDC tsunami catalog whereas multiple tsunamis may have been generated as in the case of the 2000 New Ireland earthquake sequence [*Geist and Parsons*, 2005]. Prior to the mid-20th century, there was a restricted distribution of global tide-gage stations that would indicate whether or not an earthquake was tsunamigenic at the 0.1 m threshold (i.e., "geographic censoring"). Completeness of the global catalog is estimated to begin by approximately 1952, when station distribution improved and the observation rate is approximately constant (Figure 1b). Therefore,

[1]U.S. Geological Survey, Menlo Park, California, USA.

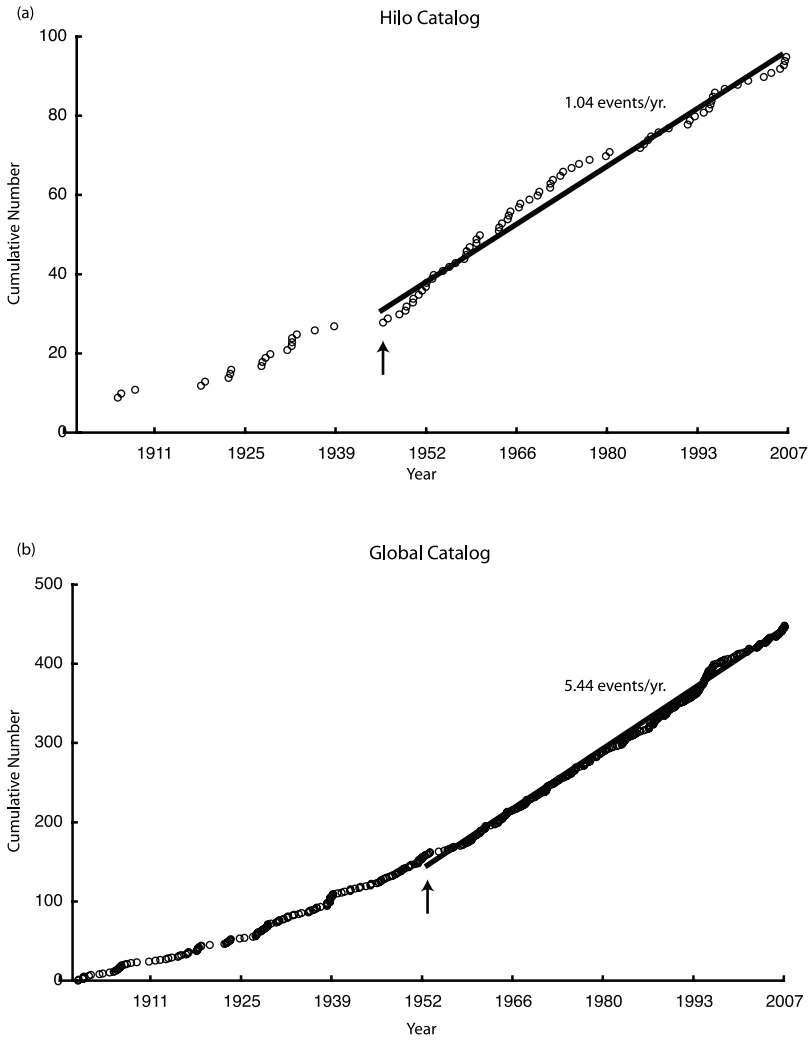

Figure 1. (a) Cumulative number of tsunami arrivals at Hilo, Hawaii since 1900. (b) Cumulative number of tsunami sources in the global NGDC catalog since 1900. Arrow represents time when the observation rate for tsunamis >0.1 m becomes approximately constant (1946 for the Hilo catalog; ~1952 for the global catalog).

the 1946–2007 catalog of tsunami arrival times at Hilo and the 1952–2007 catalog of global tsunami source times are used for the interevent analysis.

[7] To determine the empirical pdf of the interevent times ($\tau = t_{i+1} - t_i$), the data were binned according to the binning function c^n, n = 1, 2, 3, ... ($c > 1$) [*Corral*, 2004b]. The binning parameter c is chosen so as to avoid empty bins. In Figure 2, the results of using 4 different values of c are shown by the different symbols. For comparison, we also show the exponential distribution for a stationary Poisson process (heavy solid line)

$$p(\tau) = \lambda e^{-\lambda\tau}, \qquad \text{for } \tau > 0, \tag{1}$$

where the rate parameter λ is given by the ratio of the number of events to the duration of the catalog

$$\lambda = N_{cat}/T_{cat}. \tag{2}$$

For the global catalog, the empirical pdf deviates significantly from the exponential distribution at short arrival times: the Kolmogorov-Smirnov nonparametric test indicates that the Poisson null hypothesis can be rejected at the 90% confidence level. Although there is more variation in the empirical pdf for the Hilo catalog, an overabundance of short interevent times (1–10 days) is evident. In the next section, we consider different non-Poissonian distributions that statistically model the empirical interevent pdf.

3. Non-Poissonian Interevent Distribution Models

[8] We examine two different types of theoretical interevent distributions to explain the empirical pdf of tsunami interevent times shown in Figure 2. Each of these distribution types have been derived from the temporal occurrence of seismicity. The first type is a universal scaling law for long-term interevent times and the second type is based on Omori-like aftershock decay. In both cases, the interevent pdf follows a functional form of

$$p(\tau) = \lambda f(\lambda\tau) \tag{3}$$

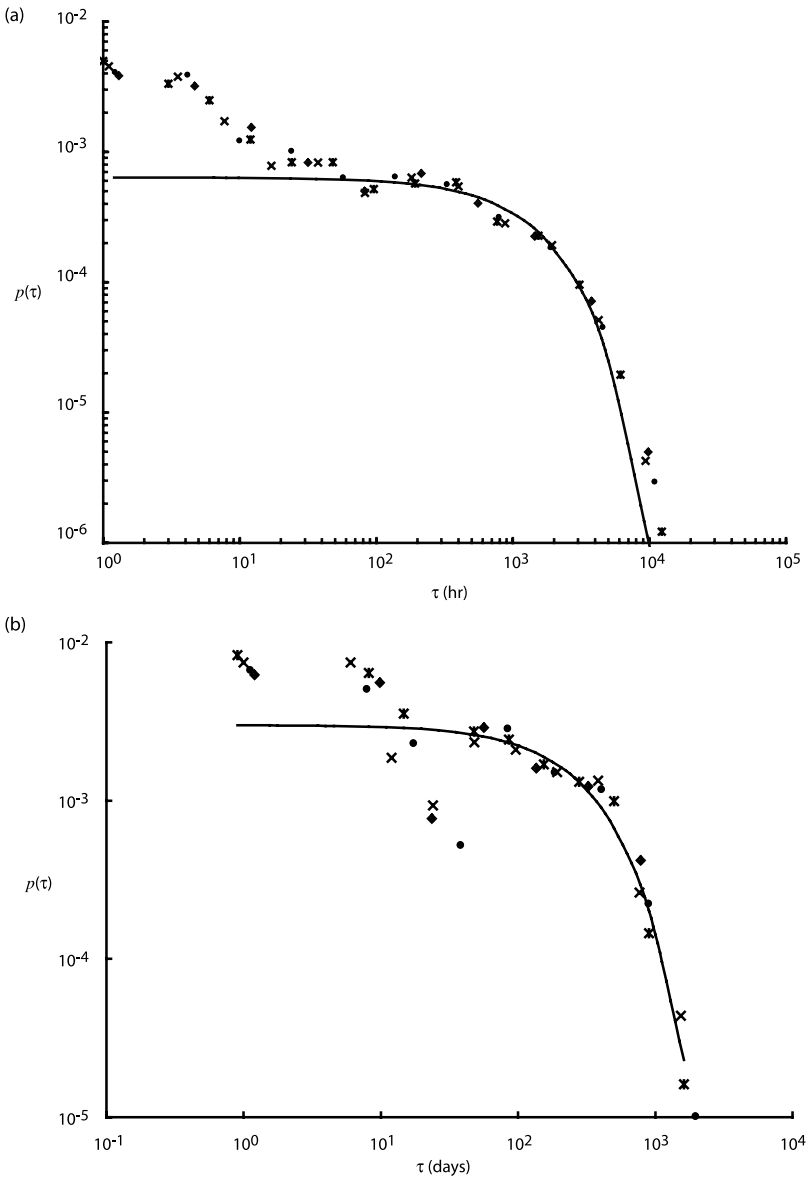

Figure 2. Empirical pdf of tsunami interevent times: (a) global catalog where symbols asterisk, cross, circle, and diamond represent four different binning parameters (c^n), where c = 2.0, 2.2, 2.4, and 2.6 hours, respectively; and (b) Hilo catalog where symbols asterisk, cross, circle, and diamond represent c = 1.8, 2.0, 2.2, and 2.4 days, respectively. Solid line represents exponential pdf based on a Poissonian model for interevent times.

[*Corral*, 2004b, 2005; *Molchan*, 2005; *Saichev and Sornette*, 2007]. The first case is for the generalized gamma distribution proposed by *Corral* [2004a] that describes stationary seismicity for time periods greater than conventional aftershock bursts:

$$f(x) = \frac{C|\delta|}{a\Gamma(\gamma/\delta)}\left(\frac{a}{x}\right)^{1-\gamma}\exp\left[-(x/a)^{\delta}\right], \qquad (4)$$

where $x = \lambda\tau$ is the nondimensional interevent time, Γ is the gamma function, C is a normalization coefficient, a is a scale parameter, and γ, δ are shape parameters of the distribution. For $\gamma < 1$, events are clustered in time, whereas for $\gamma > 1$ events behave as a quasiperiodic process. An example of the latter is the statistical model of earthquake recurrence on individual faults in Japan [*Ogata*, 1999b].

[9] A number of different catalogs were analyzed by *Corral* [2004b, 2005], including global earthquake catalogs, for which $\gamma \approx 0.7$ in most cases, suggesting universality of this distribution. The best fit distribution for the global tsunami catalog using a χ^2 minimization procedure yields γ = 0.57 – 0.60 and δ = 1.5 – 2.0 (Figure 3). An alternative procedure is to minimize *Cash*'s [1979] C statistic, which is more applicable for low-bin count data [*Nousek and Shue*, 1989]. Using this procedure, γ = 0.56 – 0.59 and δ = 1.8 – 2.4.

[10] The similar shape between earthquake and tsunami gamma distributions is expected since the source times of the global tsunami catalog are essentially a subset of the global earthquake catalog (i.e., those earthquakes that are tsunamigenic), though this is not simply a subset based on a minimum cutoff magnitude. The best fit value of γ for the

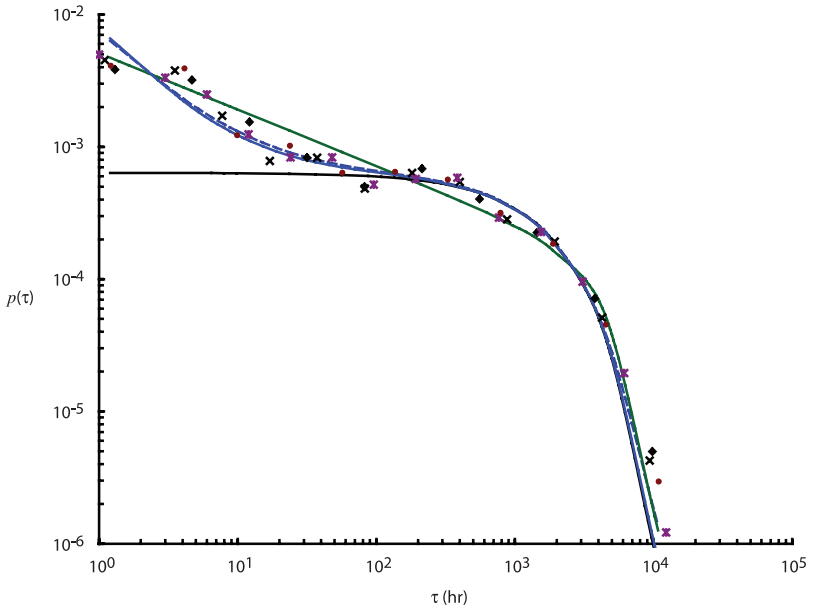

Figure 3. Three model pdfs to explain empirical distribution of tsunami interevent times (points) from the global catalog: green solid line, generalized gamma distribution for long-term correlation of events (equation (4)) [*Corral*, 2004a]; blue solid line, distribution derived from ETAS model (equation (6)) [*Saichev and Sornette*, 2007]; blue dashed line, exponential distribution augmented by a simplified form of Omori's law (equation (7)); and black solid line, exponential distribution shown for comparison. Symbols same as Figure 2a.

Hilo catalog is 0.71–0.79 (χ^2 minimization, δ = 1.3 – 1.9) and 0.73–0.79 (C statistic minimization, δ = 2.0 – 2.4), suggesting that interevent times are closer to an exponential distribution than for the global catalog. This can be explained by differences in tsunami travel times and the fact that tsunamis generated by smaller, triggered earthquakes are less likely to be recorded at a far-field station such as Hilo in comparison to the global catalog.

[11] The second type of theoretical distribution we examine is specifically associated with aftershock decay. Aftershock sequences result in a break in the universal interevent distribution (4) above. In general, the magnitude range in such a sequence is narrow such that mainshock, foreshocks, and aftershocks are not distinguished [*Kagan and Jackson*, 1999]. The nonstationary decay of an aftershock sequence as a function of time t since the mainshock is described by Omori's law such that the rate $\lambda(t)$ is given by

$$\lambda(t) = \frac{k}{(c+t)^{1+\theta}}, \tag{5}$$

where k, c and θ are nonuniversal constants. *Saichev and Sornette* [2007] explicitly develop an interevent distribution consistent with the epidemic type aftershock sequence (ETAS) model of triggered seismicity and Omori's law [*Helmstetter and Sornette*, 2002; *Kagan and Knopoff*, 1981; *Ogata*, 1999a]. In this case, the interevent distribution is based on the Omori constants c and θ and the nondimensional parameters $x = \lambda\tau$ and $\varepsilon = \lambda c$:

$$f(x) = \left[\frac{n\varepsilon^{\theta}\theta}{x^{1+\theta}} + \left(1 - n + \frac{n\varepsilon^{\theta}}{x^{\theta}}\right)^2\right]\varphi(x,\varepsilon), \tag{6}$$

where n is the ETAS branching ratio and $\varphi(x, \varepsilon)$ is a universal scaling function. *Saichev and Sornette* [2007] demonstrate that the distribution (6) is similar to Corral's universal distribution (4), except for small x in which the pdf is dominated by Omori-like decay. (Conversely, *Corral* [2004a, 2004b] indicates that a distribution similar to (4) can locally apply to aftershock bursts if the interevent times are rescaled.) At scales relevant to tsunamis, the interevent time distribution is most sensitive to variations in n and θ. For the global catalog, however, it is difficult to find a best fit if both parameters are independent. If we fix θ to a typical value of 0.1 [*Saichev and Sornette*, 2007], for example, the best fit distributions are for $n < 0.1$ (Figure 3). The apparent branching ratio n for tsunamis is significantly smaller than is found for seismicity that spans a wide range of magnitudes [*Helmstetter and Sornette*, 2002], suggesting that only the largest magnitude triggered events are tsunamigenic.

[12] The ETAS model above provides a link between earthquake sources to the empirical tsunami interevent distributions, in terms of a branching process. However, because of the difficulty in fitting distribution (6) to the relatively small amount of tsunami data (in comparison to earthquake data), a practical simplification to (6) is proposed for this study so that the number of estimated distribution parameters is reduced to one. If we assume that the Omori power law decay exponent is approximately 1 ($\theta = 0$), then the standard exponential distribution can be augmented by a t^{-1} component with a characteristic decay time T_a and normalization constant C_a as follows:

$$p(\tau) = C_a\lambda\left(e^{-\lambda\tau} + \frac{T_a}{\tau}\right). \tag{7}$$

For the global catalog the best fit T_a = 9.6 – 11.0 hours (χ^2 minimization) and T_a = 9.1 – 9.7 hours (C statistic minimization), whereas T_a = 28 – 38 hours (χ^2 minimization) and T_a = 19 – 25 hours (C statistic minimization) for the Hilo catalog (Figure 3). The distribution essentially assumes that the tsunamigenic aftershock rate can be superimposed onto a Poissonian background rate, and neglects dependence between the sources. The main purpose of this distribution, however, is to reduce the number of distribution parameters to be fit with a small sample size while capturing the inherent form of the ETAS model (Figure 3).

[13] The hazard rate function is defined as $h(\tau) \equiv p(\tau)/[1 - P(\tau)]$, where $P(\tau)$ is the cumulative distribution function. The hazard rate function can be thought of as the instantaneous failure rate or the failure probability conditional upon surviving up to time τ. For each of the model distributions, the resulting hazard rate function is characterized by an increase immediately after a tsunami and asymptotically decaying to the constant hazard rate for a Poisson process [cf. *Corral*, 2005]. This result is remarkably similar to the analysis of the Italian earthquake catalog by *Faenza et al.* [2003], using a nonparametric fit directly to the hazard rate function. Techniques to include temporal clustering into hazard assessments using the computational approach are discussed further by *Beauval et al.* [2006] and *Faenza et al.* [2007].

4. Discussion

[14] The Poisson assumption for tsunamis implies that tsunami sources are uncorrelated in time. Results from this study, however, indicate that this assumption is not valid for tsunamigenic sources at short interevent times. The statistical distributions that fit the empirical interevent data (Figure 3) suggest that triggered events are the cause for higher than expected density of short interevent times, in comparison to an exponential distribution. Because of differences in tsunami travel times, it is not immediately expected that the non-Poissonian behavior of tsunami sources is transferred to tsunami occurrence at a particular location. An examination of the Hilo tsunami catalog, however, does suggest that there is a non-Poissonian component of tsunami observations at a far-field site. The reason for this observation is that many of the triggered earthquakes that make up the abundance of short interevent times occur in close proximity to the mainshock, such that differences in tsunami travel time to a far-field station are not that significant.

[15] The triggered earthquakes, however, do not necessarily occur on the same fault as the mainshock. For example, the July 14, 1971 interplate thrust earthquake along the Solomon Islands subduction zone triggered another interplate thrust earthquake along the New Britain subduction zone 12 days later [*Schwartz et al.*, 1989], both of which were tsunamigenic. The February 2, 1965 Rat Islands interplate thrust earthquake was followed 54 days later by a tsunamigenic outer rise (normal faulting) earthquake [*Dmowska and Lovison*, 1992]. In some cases, the triggered earthquake will result in a larger local tsunami depending on differences in tsunami source parameters, contrary to the generalization that tsunamis from aftershocks are always smaller than mainshock tsunamis. For example, one of the aftershocks to the October 13, 1963 Kuril Islands M_w = 8.5 earthquake was a tsunami earthquake (M_w = 7.8 October 20, 1963) that generated significantly larger tsunami runups locally [*Pelayo and Wiens*, 1992], but smaller tsunami amplitudes at Hilo in comparison to the mainshock. Similarly (though occurring prior to the portion of the catalog analyzed in this study), a M_w = 7.9 mainshock on June 3, 1932 in central Mexico produced two tsunamigenic aftershocks (M_w = 7.8, M_s = 6.9) within 20 days. The second aftershock generated a much larger local tsunami (most likely from a concomitant landslide) than either the mainshock or the first tsunamigenic aftershock [*Farreras and Sanchez*, 1991]. Therefore, there is a significant amount of complexity among triggered earthquakes in terms of the causative mechanism and the size of the tsunamis they generate.

[16] Investigation into the possible mechanism for triggered earthquakes on a global scale has been conducted by *Parsons* [2002]. Results from that study indicated that 61% of events subsequent to and near a $M_s \geq 7.0$ earthquake were associated with positive shear stress increases. These can be considered triggered events, even though they do not necessarily occur on the same fault nor have the same mechanism as the main shock. Triggered earthquakes do appear to obey a t^{-1} Omori law decay that lasts ~7–11 years after the main shock, determined in comparison to background seismicity rates, and up to 240 km from the main shock centroid. The remaining 39% of events subsequent to and near a $M_s \geq 7.0$ earthquake were associated with shear stress decreases and mostly occurred at the same background seismicity rate. These events, therefore, are not caused (or suppressed) by the ''main shock''. There are, however, groups of earthquake described by *Parsons* [2002] associated with shear stress decrease that occur at elevated background rates persisting for 1–2 years after the main shock; these are most likely triggered by changes in normal stress, stress diffusion, or from the dynamics of seismic waves. Independent of the triggering mechanism, it does appear the most triggered events follow an Omori law aftershock decay.

5. Conclusions

[17] Analysis of tsunami source interevent times establishes that there are more short interevent times than expected from a stationary Poisson process. Deviation of the interevent distribution from exponential is also suggested at a particular coastal location (Hilo, Hawaii), although there is greater uncertainty in the site-specific distribution owing to a smaller sample size. Two statistical models are used to describe the time-clustering behavior observed in the empirical distribution. The first is a universal scaling law for the long-term temporal clustering of earthquakes [*Corral*, 2004b]. The second statistical model is based on the Omori law–like decay associated with aftershocks. Interevent distributions incorporating Omori law decay have been developed in the ETAS framework by *Saichev and Sornette* [2007]. The latter is consistent with the observation of long duration Omori-like decay of global triggered earthquakes [*Parsons*, 2002]. Specific examples of triggered events in the tsunami catalog indicate that the

triggered earthquakes do not necessarily occur on the same fault as the mainshock and that the triggered earthquake may result in a larger tsunami because of variations in tsunami source parameters. For all of the tsunami distributions examined, the hazard rate increases immediately after a tsunami and then gradually decreases asymptotically to a constant Poissonian value.

[18] **Acknowledgments.** This manuscript greatly benefited from thorough reviews by Yan Kagan, Sandy Steacy, Hal Mofjeld, Jingping Xu, and an anonymous reviewer.

References

Beauval, C., et al. (2006), Probabilistic seismic hazard estimation in low-seismicity regions considering non-Poissonian seismic occurrence, *Geophys. J. Int.*, *164*, 543–550.

Burroughs, S. M., and S. F. Tebbens (2005), Power law scaling and probabilistic forecasting of tsunami runup heights, *Pure Appl. Geophys.*, *162*, 331–342.

Cash, W. (1979), Parameter estimation in astronomy through application of the likelihood ratio, *Astrophys. J.*, *228*, 939–947.

Corral, A. (2004a), Universal local versus unified global scaling laws in the statistics of seismicity, *Physica A*, *340*, 590–597.

Corral, A. (2004b), Long-term clustering, scaling, and universality in the temporal occurrence of earthquakes, *Phys. Rev. Lett.*, *92*, 108501, doi:10.1103/PhysRevLett.1192.108501.

Corral, A. (2005), Time-decreasing hazard and increasing time until the next earthquake, *Phys. Rev. E*, *71*, 017101, doi:10.1103/PhysRevE.1171.017101.

Dmowska, R., and L. C. Lovison (1992), Influence of asperities along subduction interfaces on the stressing and seismicity of adjacent areas, *Tectonophysics*, *211*, 23–43.

Faenza, L., et al. (2003), A non-parametric hazard model to characterize the spatio-temporal occurrence of large earthquakes: An application to the Italian catalogue, *Geophys. J. Int.*, *155*, 521–531.

Faenza, L., et al. (2007), Statistical analysis of time-dependent earthquake occurrence and its impact on hazard in the low seismicity region Lower Rhine Embayment, *Geophys. J. Int.*, *171*, 797–806.

Farreras, S. F., and A. J. Sanchez (1991), The tsunami threat on the Mexican west coast: A historical analysis and recommendations for hazard mitigation, *Nat. Hazards*, *4*, 301–316.

Geist, E. L., and T. Parsons (2005), Triggering of tsunamigenic aftershocks from large strike-slip earthquakes: Analysis of the November 2000 New Ireland earthquake sequence, *Geochem. Geophys. Geosyst.*, *6*, Q10005, doi:10.1029/2005GC000935.

Geist, E. L., and T. Parsons (2006), Probabilistic analysis of tsunami hazards, *Nat. Hazards*, *37*, 277–314.

Helmstetter, A., and D. Sornette (2002), Subcritical and supercritical regimes in epidemic models of earthquake aftershocks, *J. Geophys. Res.*, *107*(B10), 2237, doi:10.1029/2001JB001580.

Kagan, Y. Y. (2002), Seismic moment distribution revisited: I. Statistical results, *Geophys. J. Int.*, *148*, 520–541.

Kagan, Y. Y., and D. D. Jackson (1999), Worldwide doublets of large shallow earthquakes, *Bull. Seismol. Soc. Am.*, *89*, 1147–1155.

Kagan, Y. Y., and L. Knopoff (1981), Stochastic synthesis of earthquake catalogs, *J. Geophys. Res.*, *86*, 2853–2862.

Molchan, G. (2005), Interevent time distribution in seismicity: A theoretical approach, *Pure Appl. Geophys.*, *162*, 1135–1150.

Nousek, J. A., and D. R. Shue (1989), χ^2 and C statistic minimization for low count per bin data, *Astrophys. J.*, *342*, 1207–1211.

Ogata, Y. (1999a), Seismicity analysis through point-process modeling: A review, *Pure Appl. Geophys.*, *155*, 471–507.

Ogata, Y. (1999b), Estimating the hazard of rupture using uncertain occurrence times of paleoearthquakes, *J. Geophys. Res.*, *104*, 17,995–18,014.

Parsons, T. (2002), Global Omori law decay of triggered earthquakes: Large aftershocks outside the classical aftershock zone, *J. Geophys. Res.*, *107*(B9), 2199, doi:10.1029/2001JB000646.

Pelayo, A. M., and D. A. Wiens (1992), Tsunami earthquakes: Slow thrust-faulting events in the accretionary wedge, *J. Geophys. Res.*, *97*, 15,321–15,337.

Pérez, O. J. (1999), Revised world seismicity catalog (1950–1997) for strong ($M_s \geq 6$) shallow ($h \leq 70$ km) earthquakes, *Bull. Seismol. Soc. Am.*, *89*, 335–341.

Saichev, A., and D. Sornette (2007), Theory of earthquake recurrence times, *J. Geophys. Res.*, *112*, B04313, doi:10.1029/2006JB004536.

Schwartz, S. Y., et al. (1989), Source process of the great 1971 Solomon Islands doublet, *Phys. Earth Planet. Inter.*, *56*, 294–310.

E. L. Geist and T. Parsons, U.S. Geological Survey, Mail Stop 999, Menlo Park, CA 94025, USA. (egeist@usgs.gov)